HHS Public Access

Author manuscript

JAMA Dermatol. Author manuscript; available in PMC 2018 January 08.

Published in final edited form as:

JAMA Dermatol. 2016 December 01; 152(12): 1335–1341. doi:10.1001/jamadermatol.2016.2997.

Use of Digitally Stained Multimodal Confocal Mosaic Images to Screen for Nonmelanoma Skin Cancer

Euphemia W. Mu, MD,
The Ronald O. Perelman Department of Dermatology, New York University School of Medicine, New York

Jesse M. Lewin, MD,
Department of Dermatology, Columbia University, New York, New York

Mary L. Stevenson, MD,
The Ronald O. Perelman Department of Dermatology, New York University School of Medicine, New York

Shane A. Meehan, MD,
The Ronald O. Perelman Department of Dermatology, New York University School of Medicine, New York

Department of Pathology, Dermatopathology Section, New York University School of Medicine, New York

John A. Carucci, MD, PhD, and
The Ronald O. Perelman Department of Dermatology, New York University School of Medicine, New York

Daniel S. Gareau, PhD, MCR
Laboratory of Investigative Dermatology, The Rockefeller University, New York, New York

Corresponding Author: Daniel S. Gareau, PhD, MCR, Laboratory of Investigative Dermatology, The Rockefeller University, 1230 York Ave, New York, NY 10065 (dgareau@mail.rockefeller.edu).

Author Contributions: Dr Mu had full access to all of the data in the study and takes responsibility for the integrity of the data and the accuracy of the data analysis.
Study concept and design: Mu, Lewin, Stevenson, Carucci, Gareau.
Acquisition, analysis, or interpretation of data: Mu, Lewin, Meehan, Carucci, Gareau.
Drafting of the manuscript: Mu, Meehan, Gareau.
Critical revision of the manuscript for important intellectual content: Mu, Lewin, Stevenson, Carucci, Gareau.
Statistical analysis: Mu, Lewin, Carucci, Gareau.
Obtaining funding: Carucci, Gareau.
Administrative, technical, or material support: Lewin, Carucci, Gareau.
Study supervision: Lewin, Carucci, Gareau.

Additional Contributions: The authors would like to thank Julie K. Karen, MD, Complete Skin & Laser Surgery, The Ronald O. Perelman Department of Dermatology, New York University School of Medicine, New York; Anna A. Bar, MD, Department of Dermatology, Oregon Health and Science University, Portland; Kishwer Nehal, MD, Department of Dermatology, Memorial Sloan Kettering Cancer Center, New York, New York; Nicholas Snavely, MD, River Place Mohs and Dermatologic Surgery Center, Oregon Health and Science University, Portland, for their contributions to this study. They received no compensation for their contributions.

Conflict of Interest Disclosures: None reported.

Additional Information: All tissue specimens imaged for this analysis were from either Memorial Sloan Kettering Cancer Center (MSKCC) or Oregon Health and Science University (OHSU). No tissue was removed from those locations to conduct this study, which used only images and took place at The Rockefeller University and New York University. The image database used for this study was created in part at OHSU and in part at MSKCC from images of their respective samples.

Abstract

IMPORTANCE—Confocal microscopy has the potential to provide rapid bedside pathologic analysis, but clinical adoption has been limited in part by the need for physician retraining to interpret grayscale images. Digitally stained confocal mosaics (DSCMs) mimic the colors of routine histologic specimens and may increase adaptability of this technology.

OBJECTIVE—To evaluate the accuracy and precision of 3 physicians using DSCMs before and after training to detect basal cell carcinoma (BCC) and squamous cell carcinoma (SCC) in Mohs micrographic surgery fresh-tissue specimens.

DESIGN—This retrospective study used 133 DSCMs from 64 Mohs tissue excisions, which included clear margins, residual BCC, or residual SCC. Discarded tissue from Mohs surgical excisions from the dermatologic surgery units at Memorial Sloan Kettering Cancer Center and Oregon Health & Science University were collected for confocal imaging from 2006 to 2011. Final data analysis and interpretation took place between 2014 and 2016. Two Mohs surgeons and a Mohs fellow, who were blinded to the correlating gold standard frozen section diagnoses, independently reviewed the DSCMs for residual nonmelanoma skin cancer (NMSC) before and after a brief training session (about 5 minutes). The 2 assessments were separated by a 6-month washout period.

MAIN OUTCOMES AND MEASURES—Diagnostic accuracy was characterized by sensitivity and specificity of detecting NMSC using DSCMs vs standard frozen histopathologic specimens. The diagnostic precision was calculated based on interobserver agreement and κ scores. Paired 2-sample *t* tests were used for comparative means analyses before and after training.

RESULTS—The average respective sensitivities and specificities of detecting NMSC were 90% (95% CI, 89%-91%) and 79% (95% CI, 52%-100%) before training and 99% (95% CI, 99%-99%) ($P = .001$) and 93% (95% CI, 90%-96%) ($P = .18$) after training; for BCC, they were 83% (95% CI, 59%-100%) and 92% (95% CI, 81%-100%) before training and 98% (95% CI, 98%-98%) ($P = .18$) and 97% (95% CI, 95%-100%) ($P = .15$) after training; for SCC, they were 73% (95% CI, 65%-81%) and 89% (95% CI, 72%-100%) before training and 100% ($P = .004$) and 98% (95% CI, 95%-100%) ($P = .21$) after training. The pretraining interobserver agreement was 72% ($\kappa = 0.58$), and the posttraining interobserver agreement was 98% ($\kappa = 0.97$) ($P = .04$).

CONCLUSIONS AND RELEVANCE—Diagnostic use of DSCMs shows promising correlation to frozen histologic analysis, but image quality was affected by variations in image contrast and mosaic-stitching artifact. With training, physicians were able to read DSCMs with significantly improved accuracy and precision to detect NMSC.

Over 5 million cases of nonmelanoma skin cancer (NMSC) are diagnosed annually in the United States, with a 35% increase in incidence between 2006 and 2012.[1] The growing cost of NMSC to the health care system compels the refinement of current diagnostic and treatment techniques. Confocal microscopy, introduced to clinical dermatology in 1991, has the potential to provide more rapid bedside pathologic analysis by producing images with subcellular resolution without physical sectioning.[2-4] However, the clinical implementation of confocal microscopy is impeded in part by differences between traditional grayscale

confocal images and histopathologic slides requiring physician retraining for accurate interpretation.[3,5-8]

To recapitulate standard histologic analysis and promote adaptability of confocal images, we created digitally stained confocal mosaics (DSCMs) using multimodal microscopy (Figure 1).[6,9,10] These mosaics mimicked histologic features, including high resolution to examine cell structure, large fields of view to analyze tissue architecture, and contrasting imaging modes to highlight morphologic characteristics. Small, high-resolution fields of view were stitched together to produce mosaics in reflectance mode.[11] Fluorescence mode was added to image acridine orange contrast of stained nuclei.[12] In a prior study,[7] 2 Mohs surgeons detected basal cell carcinoma (BCC) using confocal fluorescent microscopy with a sensitivity of 97% and specificity 89% in 149 submosaics.

While BCC has a high nuclear-to-cytoplasmic ratio,[13] squamous cell carcinoma (SCC) cannot be as easily diagnosed with a single fluorescent nuclear stain. A multimodal microscope was subsequently developed to image 3 independent modes: acridine orange fluorescence (Figure 2A), eosin fluorescence (Figure 2B), and endogenous reflectance (Figure 3A).[10] These 3 signals mark the presence of nuclei, cytoplasm, and extracellular components (such as collagen and keratin), respectively. The addition of the cytoplasmic contrast by eosin fluorescence enhanced the cytoplasmic details that were useful in screening for SCC.[10] In a pilot investigation using DSCMs produced from a trimodal confocal microscope, 2 Mohs surgeons identified SCC with 100% sensitivity and 90% specificity in 10 mosaics.[10]

Digital staining was incorporated pixel by pixel by mathematically translating the input of light intensities from the 3 microscopy modes into 3 outputs of red, green, and blue levels to produce a pink-and-purple image similar to that of a routine histologic slide stained with hematoxylin-eosin (Figure 3B).[6] The confocal images converted dark-field images, in which bright nuclei appeared in grayscale on a black background, into a bright-field image, in which digitally colored structures were displayed on a white background.

To our knowledge, this is the first study to evaluate the use of DSCMs to differentiate BCC, SCC, and negative margins in Mohs specimens. The primary aim was to assess the sensitivity and specificity of interpreting DSCMs before and after brief training in the technique. The interobserver agreement was also determined before and after training.

Methods

Tissue Collection and Preparation

Mohs surgical excisions from the dermatologic surgery units at Memorial Sloan Kettering Cancer Center and Oregon Health & Science University were performed, and discarded tissue was collected for confocal imaging from 2006 to 2011. Final data analysis and interpretation took place between 2014 and 2016. Each frozen specimen was thawed, rinsed with isotonic saline, stained with 1mM acridine orange (pH, 6.0)[12] or the combination of 1mM acridine orange (pH, 6.0) and eosin (pH, 6.0),[10] rinsed again with isotonic saline, and

imaged with confocal mosaicing microscopy, as previously described.[10,12] This study was approved by the institutional review board at the New York University School of Medicine.

Fluorescent Nuclear Contrast

A modified version of a commercial Vivascope 2000 confocal laser-scanning microscope (Caliber ID Inc) served as the prototype for capturing initial mosaic images.[11,12,14] A 488-nm argon-ion laser was used to illuminate tissue, and resultant fluorescence emission was detected in the range 500 to 600 nm. The tissue was mounted, and a set of 2-dimensional images of the tissue surface was captured using a magnification ×30, 0.9 numerical aperture customized water-immersion objective lens (StableView; Lucid Inc). The images were then digitally stitched together with a Matlab-based software algorithm (The MathWorks Inc) to create a consolidated confocal mosaic.[12] The mosaic field of view corresponded to light microscope magnification ×2.

Multimodal Confocal Microscopy

Mosaic images were produced using a modified trimodal confocal microscope that combined 3 imaging modes: acridine orange fluorescence to label nuclei, eosin fluorescence to indicate cytoplasm, and endogenous reflectance to identify collagen and keratin.[10] An augmented version of the VivaScope 2500 microscope (Lucid) was enhanced with a 30-mW, 488-nm diode laser (Blue Sky Research) and a 50-mW, 532-nm diode laser (Lasermate Group Inc), which were linked with a dichroic filter (Semrock Inc). Switching between the excitation wavelengths of 488 and 532 nm for acridine orange and eosin fluorescence, respectively, produced absorption contrast between acridine orange and eosin. The sum of the eosin and reflectance signals was digitally stained pink to mimic the appearance of eosin in standard histologic specimens. The acridine orange mosaic was shaded purple to imitate the appearance of hematoxylin in standard specimens.

Study Sample and Design

Mosaics from 64 Mohs tissue samples were divided into 2 to 4 smaller submosaics to show morphologic characteristics at higher resolution and magnification (Figure 4). All images were reviewed by a dermatopathologist (S.A.M.), and images with poor correlation to the frozen diagnosis were removed from the final study set, which included 133 submosaics. Three physicians, all blinded to the frozen section diagnoses and interpretations of other physicians, independently diagnosed each DSCM as having clear margins, BCC, or SCC. The 3 physicians included 2 Mohs surgeons (J.M.L. and J.A.C.) and a Mohs fellow (M.L.S.). The confocal submosaics were displayed in a random order at magnification ×2 to ×4 on a 30-inch flat-screen monitor (Apple Cinema Display). Mimicking pathologic examination, images could be magnified up to ×30. The participating physicians compiled their diagnoses and comments in an Excel database (Microsoft). These answers were compared with the original Mohs maps drawn by the Mohs surgeons at the time of surgery. After a washout period of 6 months (prior studies evaluating histopathologic diagnostic accuracy have used washout periods ranging from 1 to 3 weeks[15-17]), the 3 physicians were given a brief training session that involved reviewing features of 6 example slides in 5 minutes (eAppendix in the Supplement) and asked to regrade the study set.

Statistical Analysis

Statistical analyses were performed in Stata 11.0 for Mac (StataCorp LP). In the analyses inclusive of all NMSC subtypes, true positive was defined as the presence of tumor in both the frozen section and confocal images; true negative as no tumor in both; false positive as the presence of tumor on confocal imaging but no tumor on frozen; and false negative as tumor not observed on confocal imaging, but the presence of tumor on frozen sections.

In analyses by cancer subtype, true positive indicated matched tumor type identified on frozen sections and sub-mosaics; false positive indicated presence of tumor on sub-mosaics but no identifiable tumor or a different tumor type on frozen section; false negative designated no tumor or different tumor type on confocal imaging, but the presence of the specific tumor type on frozen section. The true negative definition remained the same as for generic NMSC.

Sensitivity and specificity were calculated before and after training sessions. The interobserver agreement and κ values were calculated before and after training sessions: κ values less than 0.40 indicated slight to fair agreement; κ values from 0.41 to 0.60, moderate agreement; κ values from 0.61 to 0.80, substantial agreement; and κ values from 0.81 to 0.99, nearly perfect agreement.[18] A paired 2-sample *t* tests was used for comparative means analyses of sensitivity, specificity, and interobserver agreement.

Results

Of the total 133 DSCMs, 44 (33%) contained residual BCC; 32 (24%), SCC; and 57 (43%), clear margins. Each mosaic was produced in an average of 9 minutes. An example of a DSCM and the corresponding hematoxylin-eosin-stained Mohs frozen section are shown in Figure 1.

Prior to training, the average sensitivity and specificity of detecting residual carcinoma by DSCM were 90% (95% CI, 89%-91%) and 79% (95% CI, 52%-100%), respectively (Table). After training, the average sensitivity and specificity of detecting residual carcinoma were 99% (95% CI, 99%-99%) ($P = .001$) and 93% (95% CI, 90%-96%) ($P = .18$), respectively.

By cancer type, the pretraining sensitivity and specificity for BCC were 83% (95% CI, 59%-100%) and 92% (95% CI, 81%-100%), respectively; for SCC, 73% (95% CI, 65%-81%) and 89% (95% CI, 72%-100%), respectively. The posttraining sensitivity and specificity for BCC were 98% (95% CI, 98%-98%) ($P = .18$) and 97% (95% CI, 95%-100%) ($P = .15$), respectively; for SCC, 100% ($P = .004$) and 98% (95% CI, 95%-100%) ($P = .21$), respectively. No trends were identified by years of experience with Mohs training and diagnostic accuracy.

Comparing agreement among the 3 physicians, we found that the diagnostic concordance before training was 72% (95% CI, 54%-91%; $\kappa = 0.58$), and after training it was 98% (95% CI, 97%-99%; $\kappa = 0.97$) ($P = .04$).

Discussion

Advances in confocal technology may expedite Mohs micrographic surgery for treatment of NMSC. To our knowledge, this is the first study to assess DSCMs for screening both SCC and BCC in Mohs excisions. With training, the physicians detected NMSC on DSCM with a high sensitivity (99%) and specificity (93%), which approximates the accuracy required for the excellent cure rate of Mohs surgery.[19-21] Notably, there was a statistically significant improvement in sensitivity for detecting NMSC after training, which can largely be attributed to the SCC subset. By cancer subtypes, BCC and SCC were both accurately diagnosed after training on DSCMs, findings which were comparable to prior confocal studies separately studying BCC[7] and SCC.[10]

Traditional grayscale confocal microscopy requires specialized training to interpret, which can be an impediment to adaptation of the technology.[6-8,22] Prior studies have reported training periods ranging from 30-minute oral presentations[22,23] to at least 2 months of confocal experience[6,7] and found that training improved accuracy and interobserver agreement.[24] Application of digital stains to more closely mimic the appearance of frozen histologic slides reduces the amount of physician retraining needed. The training in this study lasted minutes, which is shorter than that reported in prior studies, and resulted in a significant increase in the accuracy and precision of reading DSCMs. Seeing examples of each diagnosis in the training slides allowed the physicians to recognize similar patterns in the study set. In particular, the sensitivity of identifying SCC improved after training as the physicians learned to identify the distinct appearance of irregularly shaped aggregates of atypical keratinocytes with squamous pearls on DSCMs.

This study had a number of limitations Of all the submosaics generated, 29% were removed from the study owing to uninterpretable image quality, which was determined by a dermatopathologist. The eliminated images would be comparable to frozen slides that the Mohs surgeon would ask to be recut in a clinical setting. Since this was not possible in the study, the uninterpretable images were removed to maintain integrity of the study set evaluated. In addition, while digital staining reduces the training time required, some instruction is still necessary for optimal diagnostic accuracy using DSCMs. In contrast to frozen histologic analysis, the submosaics in this study were noted to have uneven image contrast and mosaicing artifact. Inconsistent contrast staining can result from irregular diffusion of stains into tissue, focal plane differences, and uneven specimen positioning on the glass platform. Moreover, stitching within mosaics is necessary to create images with both a greater field of view and higher cellular resolution. However, stitching can generate duplicate structures or obscure morphologic characteristics. These technical limitations inherent to the available technology are being addressed to better adapt confocal microscopy for future clinical use.

Conclusions

Confocal microscopy in dermatology has undergone impressive advances over the past 2 decades. The incorporation of digital staining to mimic histopathologic appearance reduces but does not yet eliminate the need for physician retraining to screen BCC and SCC in Mohs

excisions. Future developments in confocal microscopy will further improve the adaptability in confocal technology in dermatologic surgery.

Supplementary Material

Refer to Web version on PubMed Central for supplementary material.

Acknowledgments

Funding/Support: This study analyzed SCC images from work supported by National Institutes of Health (NIH) grant 5-T32-CA106195 and BCC images from work supported by NIH grant R01EB002715. Support for this work was provided by the Rockefeller University's Robertson Therapeutics Development fund and NIH grant 1R01CA193390-01.

Role of the Funder/Sponsor: The funders had no role in the design and conduct of the study; collection, management, analysis, and interpretation of the data; preparation, review, or approval of the manuscript; and decision to submit the manuscript for publication.

References

1. Rogers HW, Weinstock MA, Feldman SR, Coldiron BM. Incidence estimate of nonmelanoma skin cancer (keratinocyte carcinomas) in the US population. JAMA Dermatol. 2012; 151(10):1081–1086.
2. Rajadhyaksha M, Grossman M, Esterowitz D, Webb RH, Anderson RR. In vivo confocal scanning laser microscopy of human skin: melanin provides strong contrast. J Invest Dermatol. 1995; 104(6): 946–952. [PubMed: 7769264]
3. Ulrich M, Lange-Asschenfeldt S. In vivo confocal microscopy in dermatology: from research to clinical application. J Biomed Opt. 2013; 18(6):061212. [PubMed: 23338938]
4. New KC, Petroll WM, Boyde A, et al. In vivo imaging of human teeth and skin using real-time confocal microscopy. Scanning. 1991; 13(5):369–372.
5. González S. Confocal reflectance microscopy in dermatology: promise and reality of non-invasive diagnosis and monitoring. Actas Dermosifiliogr. 2009; 100(suppl 2):59–69. [PubMed: 20096164]
6. Gareau DS. Feasibility of digitally stained multimodal confocal mosaics to simulate histopathology. J Biomed Opt. 2009; 14(3):034050. [PubMed: 19566342]
7. Karen JK, Gareau DS, Dusza SW, Tudisco M, Rajadhyaksha M, Nehal KS. Detection of basal cell carcinomas in Mohs excisions with fluorescence confocal mosaicing microscopy. Br J Dermatol. 2009; 160(6):1242–1250. [PubMed: 19416248]
8. Que SK, Fraga-Braghiroli N, Grant-Kels JM, Rabinovitz HS, Oliviero M, Scope A. Through the looking glass: basics and principles of reflectance confocal microscopy. J Am Acad Dermatol. 2015; 73(2):276–284. [PubMed: 26051696]
9. Gareau DS, Jeon H, Nehal KS, Rajadhyaksha M. Rapid screening of cancer margins in tissue with multimodal confocal microscopy. J Surg Res. 2012; 178(2):533–538. [PubMed: 22721570]
10. Gareau D, Bar A, Snaveley N, et al. Tri-modal confocal mosaics detect residual invasive squamous cell carcinoma in Mohs surgical excisions. J Biomed Opt. 2012; 17(6):066018. [PubMed: 22734774]
11. Patel YG, Nehal KS, Aranda I, Li Y, Halpern AC, Rajadhyaksha M. Confocal reflectance mosaicing of basal cell carcinomas in Mohs surgical skin excisions. J Biomed Opt. 2007; 12(3): 034027. [PubMed: 17614735]
12. Gareau DS, Li Y, Huang B, Eastman Z, Nehal KS, Rajadhyaksha M. Confocal mosaicing microscopy in Mohs skin excisions: feasibility of rapid surgical pathology. J Biomed Opt. 2008; 13(5):054001. [PubMed: 19021381]
13. Gareau DS, Karen JK, Dusza SW, Tudisco M, Nehal KS, Rajadhyaksha M. Sensitivity and specificity for detecting basal cell carcinomas in Mohs excisions with confocal fluorescence mosaicing microscopy. J Biomed Opt. 2009; 14(3):034012. [PubMed: 19566305]

14. Chung VQ, Dwyer PJ, Nehal KS, et al. Use of ex vivo confocal scanning laser microscopy during Mohs surgery for nonmelanoma skin cancers. Dermatol Surg. 2004; 30(12, pt 1):1470–1478. [PubMed: 15606734]
15. Pantanowitz L, Sinard JH, Henricks WH, et al. College of American Pathologists Pathology and Laboratory Quality Center. Validating whole slide imaging for diagnostic purposes in pathology: guideline from the College of American Pathologists Pathology and Laboratory Quality Center. Arch Pathol Lab Med. 2013; 137(12):1710–1722. [PubMed: 23634907]
16. Evered A, Dudding N. Accuracy and perceptions of virtual microscopy compared with glass slide microscopy in cervical cytology. Cytopathology. 2011; 22(2):82–87. [PubMed: 20482714]
17. Nielsen PS, Lindebjerg J, Rasmussen J, Starklint H, Waldstrøm M, Nielsen B. Virtual microscopy: an evaluation of its validity and diagnostic performance in routine histologic diagnosis of skin tumors. Hum Pathol. 2010; 41(12):1770–1776. [PubMed: 20869750]
18. Viera AJ, Garrett JM. Understanding interobserver agreement: the kappa statistic. Fam Med. 2005; 37(5):360–363. [PubMed: 15883903]
19. Leibovitch I, Huilgol SC, Selva D, Richards S, Paver R. Basal cell carcinoma treated with Mohs surgery in Australia, II: outcome at 5-year follow-up. J Am Acad Dermatol. 2005; 53(3):452–457. [PubMed: 16112352]
20. Rowe DE, Carroll RJ, Day CL Jr. Long-term recurrence rates in previously untreated (primary) basal cell carcinoma: implications for patient follow-up. J Dermatol Surg Oncol. 1989; 15(3):315–328. [PubMed: 2646336]
21. Rowe DE, Carroll RJ, Day CL Jr. Prognostic factors for local recurrence, metastasis, and survival rates in squamous cell carcinoma of the skin, ear, and lip: implications for treatment modality selection. J Am Acad Dermatol. 1992; 26(6):976–990. [PubMed: 1607418]
22. Liu J, Li M, Li Z, et al. Learning curve and interobserver agreement of confocal laser endomicroscopy for detecting precancerous or early-stage esophageal squamous cancer. PLoS One. 2014; 9(6):e99089. [PubMed: 24897112]
23. Gerger A, Koller S, Kern T, et al. Diagnostic applicability of in vivo confocal laser scanning microscopy in melanocytic skin tumors. J Invest Dermatol. 2005; 124(3):493–498. [PubMed: 15737188]
24. Talreja JP, Turner BG, Gress FG, et al. Pre- and post-training session evaluation for interobserver agreement and diagnostic accuracy of probe-based confocal laser endomicroscopy for biliary strictures. Dig Endosc. 2014; 26(4):577–580. [PubMed: 24344750]

Key Points

Question

What are the diagnostic sensitivity and specificity of digitally stained confocal mosaic images to detect basal cell carcinoma and squamous cell carcinoma in Mohs tissue specimens before and after very brief training in use of the technique?

Findings

In this retrospective study using 133 digitally stained confocal mosaics from 64 Mohs tissue excisions, the average respective sensitivities and specificities for detecting nonmelanoma skin cancer among 3 physicians were 90% and 79% prior to training and 99% and 93% after training.

Meaning

Digitally staining confocal images reduced but did not eliminate the retraining necessary to allow Mohs surgeons to detect nonmelanoma skin cancer with high sensitivity and specificity.

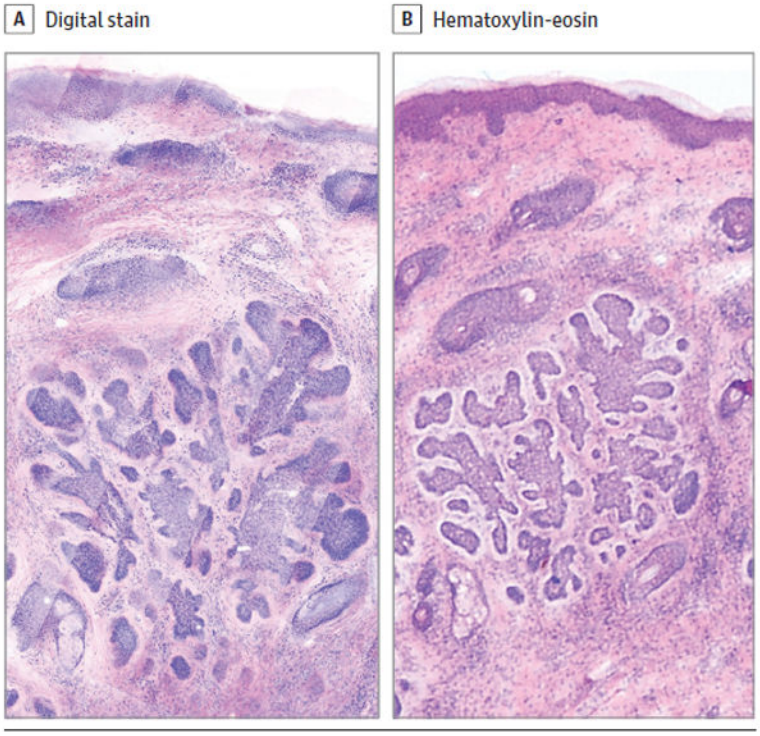

Figure 1. Comparison of a Digitally Stained Confocal Mosaic and Corresponding Hematoxylin-Eosin–Stained Mohs Frozen Section

A, Digitally stained confocal mosaic of basal cell carcinoma. B, Corresponding hematoxylin-eosin–stained Mohs frozen section. The lateral field of view is 2.25mm(original magnification ×30 for both). The acridine orange fluorescent contrast and hematoxylin highlight nuclear material in confocal and frozen sections, respectively. The reflectance contrast and eosin denote the cytoplasmic material in confocal and frozen sections, respectively.

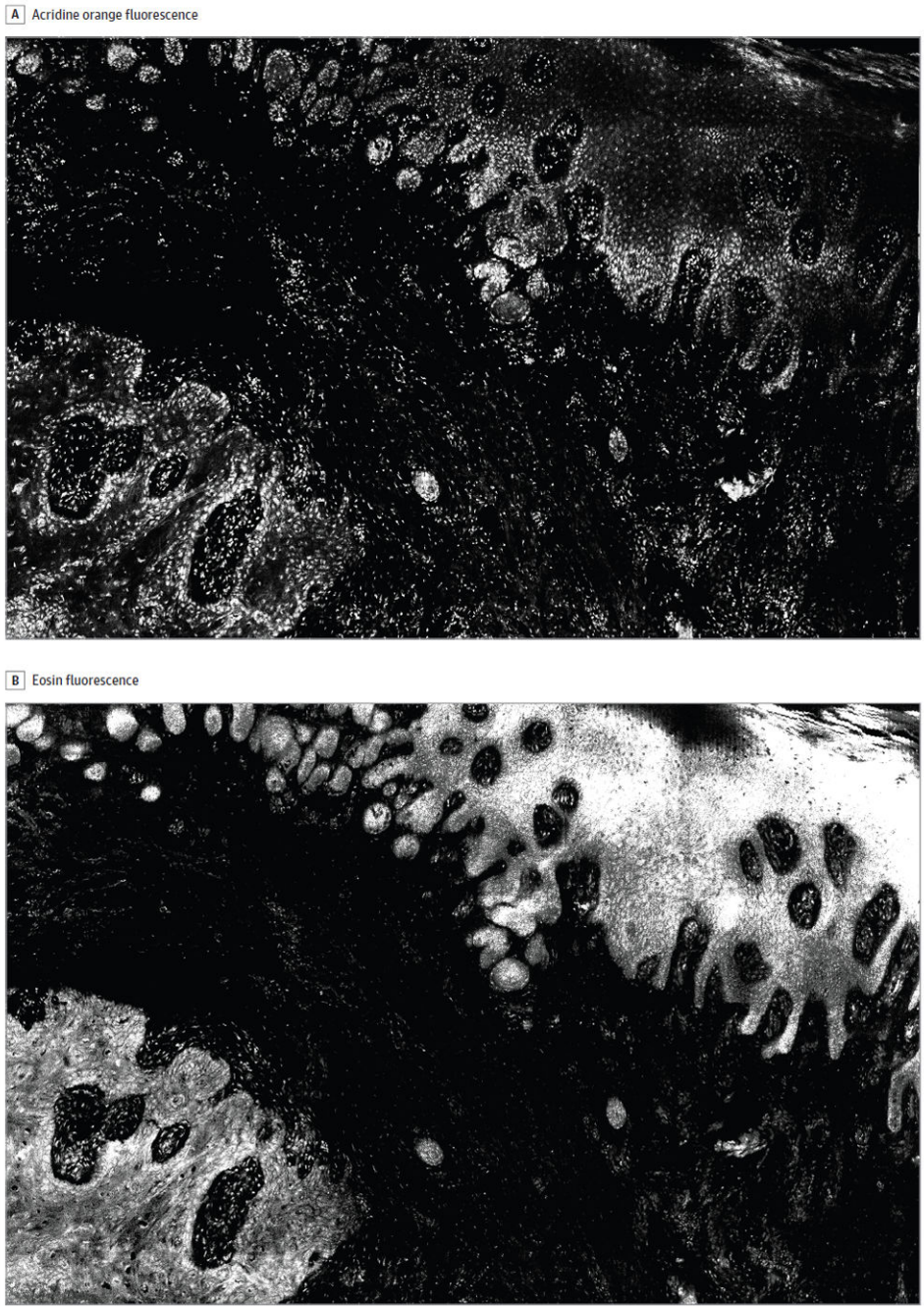

Figure 2. Trimodal Digitally Stained Confocal Mosaic Images of Invasive Squamous Cell Carcinoma, Part 1: Fluorescence Modes

The images include an acridine orange fluorescence mode to highlight nuclei (A) and an eosin fluorescence mode to demarcate cytoplasmic structures (B). The lateral field of view is 4 mm.

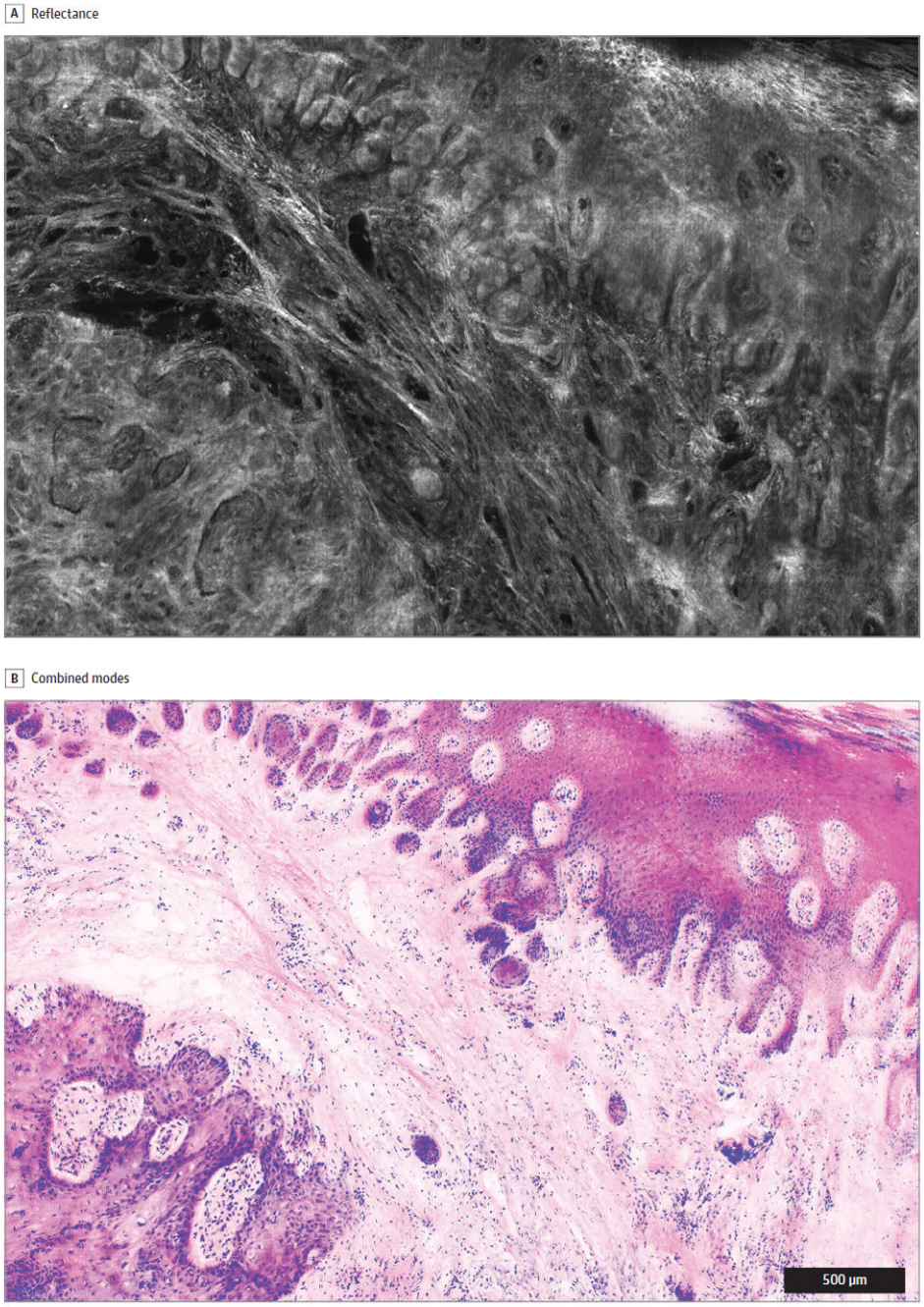

Figure 3. Trimodal Digitally Stained Confocal Mosaic Images (DSCMs) of Invasive Squamous Cell Carcinoma, Part 2: Reflectance and DSCM Modes

The images include a reflectance mode to show collagen and keratin (A) and the final mosaic DSCM (B), which combines the 2 modes from Figure 2 plus eosin fluorescence from panel A. The lateral field of view is 4 mm.

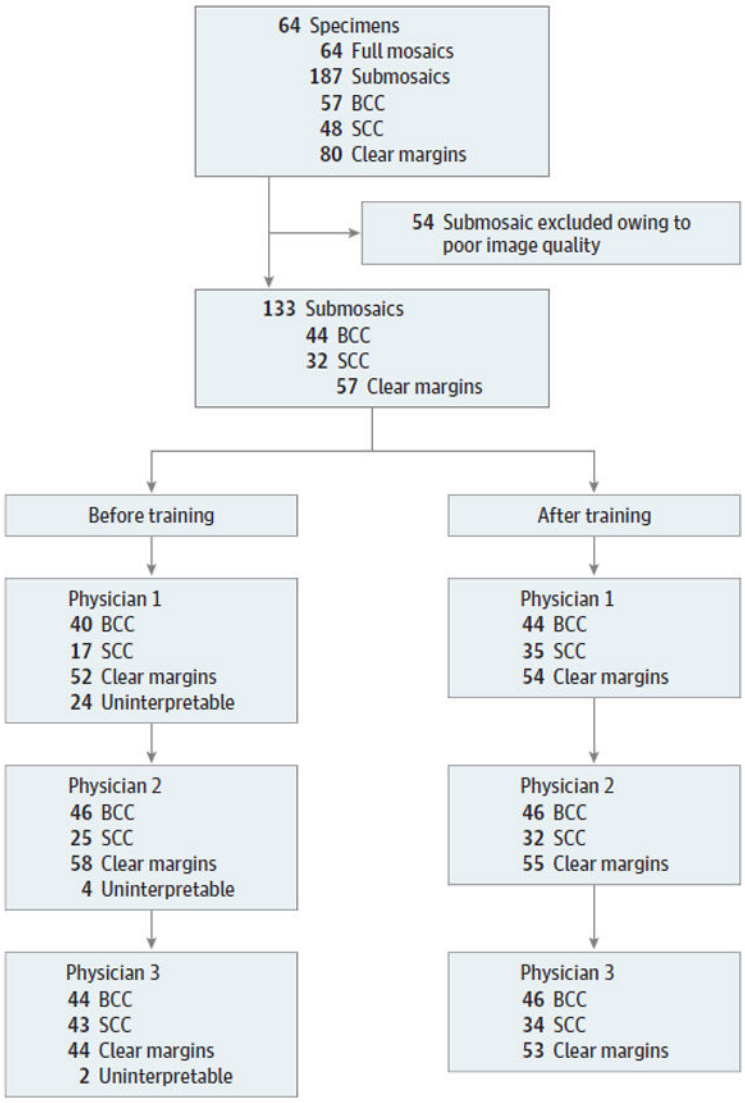

Figure 4. Diagram of the Selection Process for Submosaics Included in the Study Set

The 64 full mosaics imaged from 64 specimens were divided into 187 total submosaics. Of these, 54 were eliminated owing to poor image quality. The final study set included 133 submosaics. Participating physician assessments before and after training are listed. BCC indicates basal cell carcinoma; SCC, squamous cell carcinoma.

Table

Mean NMSC Sensitivity and Specificity Achieved by the 3 Participating Physicians Using DSCMs Before and After Training

	All NMSC (n = 76)			BCC (n = 44)			SCC (n = 32)		
Characteristic	**Before**	**After**	***P* Value**	**Before**	**After**	***P* Value**	**Before**	**After**	***P* Value**
Sensitivity, %	90	99	.001[a]	83	98	.18	73	100	.004[a]
Specificity, %	79	93	.18	92	97	.15	89	98	.21

Abbreviations: BCC, basal cell carcinoma; DSCMs, digitally stained confocal mosaic images; NMSC, nonmelanoma skin cancer; SCC, squamous cell carcinoma.

[a] $P < .05$ indicates a statistically significant difference.